

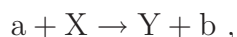
Chapter 17

Nuclear Reactions

Note to students and other readers: This Chapter is intended to supplement Chapter 11 of Krane's excellent book, "Introductory Nuclear Physics". Kindly read the relevant sections in Krane's book first. This reading is supplementary to that, and the subsection ordering will mirror that of Krane's, at least until further notice.

17.1 Types of Reactions and Conservation Laws

A typical nuclear reaction is depicted in Figure 17.1. The following two ways of describing that reaction are equivalent:



or



From now on, we shall usually use the latter because it is more compact (and easier to type!).

The above reaction is the kind we shall focus on because they represent most of the important reactions in Nuclear Physics and Engineering and the Radiological Sciences. There are only two bodies in the final state: a and Y . The particle labelled " a " is the projectile. We will generally restrict ourselves to considering light projectiles, with $A \leq 4$, and projectile energies, $T_a \lesssim 10$ MeV. The particle labelled " X " is to be thought of as the "target". The particle labelled " b " is generally the lighter reaction product, and is often the particle that is observed by the measurement apparatus. The remaining reaction product, is " Y ". The is generally the heavier of the two reaction products, and is usually unobserved, as it stays within the target "foil".

Figure 17.1: A typical nuclear reaction.

Some nomenclature

reaction	name	example
$X(a,\gamma)Y$	<i>radiative capture</i>	${}^A_ZX_N(n,\gamma){}^{A+1}_ZX_{N+1}$
$X(\gamma,b)Y$	<i>nuclear photoeffect</i>	${}^A_ZX_N(\gamma,p){}^{A-1}_ZX_N$
$X(a,a)X$	<i>nuclear scattering</i>	${}^A_ZX_N(\alpha,\alpha){}^A_ZX_N$, Rutherford scattering
$X(a,a)X^*$	<i>inelastic scattering</i>	${}^A_ZX_N(n,n){}^A_ZX_N^*$
	<i>knock out reaction</i>	${}^A_ZX_N(n,nn){}^A_ZX_{N-1}$, ${}^A_ZX_N(n,np){}^A_{Z-1}X_N$
	<i>transfer reaction</i>	${}^A_ZX_N(n,p){}^A_{Z-1}X_{N+1}$
	<i>direct reactions</i>	“a” interacts with only one or a few nucleons in X
	<i>compound reactions</i>	$a + X \rightarrow Y^m_{t_{1/2} \gg \sim 10^{-23}\text{s}} \rightarrow \text{fragments}$
	<i>resonance reaction</i>	$n \text{ or } p + X \rightarrow Y^m \rightarrow \text{decay products}$

17.1.1 Observables

Returning back to an $X(a,b)Y$ reaction, the most comprehensive experiment one can perform is to determine the b-particle type, and map out its angular distribution pattern, a so-called 4π experiment. At each different angle, we also measure T_b , because that can change with direction as well. Refer to Figure 17.2.

Figure 17.2: A typical set-up for a 4π experiment.

By knowing the intensity of the beam, we can thus compute the differential cross section, differential in T_b , θ_b , and ϕ_b , presented here in the 3 different forms that one encounters in the literature.

$$\frac{d\sigma(T_b, \theta_b, \phi_b)}{d\Omega_b dT_b} = \frac{d\sigma}{d\Omega_b dT_b} = \sigma(T_b, \theta_b, \phi_b) , \quad (17.1)$$

where $d\Omega_b$ is the differential solid angle associated with the direction of the b-particle, namely:

$$d\Omega_b = \sin \theta_b d\theta_b d\phi_b .$$

The third form is favored by some authors (not me) because of its brevity. However, its use is common, and I wanted to familiarize you with it.

From this differential cross section, alternative, integrated forms may be found:

the cross section differential in angles only,

$$\sigma(\theta_b, \phi_b) = \frac{d\sigma}{d\Omega_b} = \frac{d\sigma(\theta_b, \phi_b)}{d\Omega_b} = \int dT_b \left(\frac{d\sigma(T_b, \theta_b, \phi_b)}{d\Omega_b dT_b} \right) , \quad (17.2)$$

the cross section differential in energy only,

$$\sigma(T_b) = \frac{d\sigma}{dT_b} = \frac{d\sigma(T_b)}{dT_b} = \int d\Omega_b \left(\frac{d\sigma(T_b, \theta_b, \phi_b)}{d\Omega_b dT_b} \right) , \quad (17.3)$$

and the total cross section,

$$\sigma = \int dT_b \int d\Omega_b \left(\frac{d\sigma(T_b, \theta_b, \phi_b)}{d\Omega_b dT_b} \right) . \quad (17.4)$$

If one normalize (17.1) as follows:

$$p(T_b, \theta_b, \phi_b) = \frac{1}{\sigma} \frac{d\sigma(T_b, \theta_b, \phi_b)}{d\Omega_b dT_b} , \quad (17.5)$$

$p(T_b, \theta_b, \phi_b)$ is a “joint” probability distribution, properly normalized, over the variables, T_b , θ_b , and ϕ_b . From this probability distribution, we can determine quantities like, $\overline{T_b}$, the average energy, or $1 - \cos \overline{\theta_b}$, the so-called *scattering power*.

17.1.2 Conservation laws

The conservation laws are essential tools in scattering analysis. Conservation of energy and linear momentum allow us to deduce the properties of X and Y. Conservation of neutron and proton number also helps us deduce the properties of X and Y. Conservation of angular momentum and parity, allow us to deduce spins and parities.

17.2 Energetics of Nuclear Reactions

General Considerations in a Relativistic Formalism

For the X(a,b)Y reaction, conservation of Total Energy means:

$$m_a c^2 + m_x c^2 + T_a + T_X = m_b c^2 + m_y c^2 + T_b + T_Y , \quad (17.6)$$

or,

$$Q + T_a + T_X = T_b + T_Y , \quad (17.7)$$

where,

$$Q \equiv (m_a + m_x - [m_b + m_y])c^2 . \quad (17.8)$$

Q is the *reaction Q-value*. When $Q > 0$, the reaction is exothermic (or exoergic). Energy is released by the transformation. When $Q < 0$, the reaction is endothermic (or endoergic). Energy is required, by the kinetic energies of the initial reactants, to make the transformation “go”.

Recall that (17.7) is a relativistic expression. Therefore, we should use relativistic expressions for the kinetic energies. Doing so,

$$T_{\text{rel}} = mc^2(\gamma - 1) . \quad (17.9)$$

Since the maximum energy projectile we deal with is about 10 MeV, we have the situation where $T \ll mc^2$. Thus we can find a relationship that relates T_{rel} , to its non-relativistic counterpart, T_{NR} :

$$T_{\text{rel}} = T_{\text{NR}}[1 + \frac{3}{4}\beta^2 + \mathcal{O}(\beta^4)] . \quad (17.10)$$

In the worst possible case ($T = 10$ MeV, $m_i = m_p$, the relativistic correction amounts to:

$$\frac{3}{4}\beta^2 \cong \frac{3T}{2m_p c^2} \cong 0.015 . \quad (17.11)$$

Therefore, in the worst possible $Q = 0$ case, there is a 1.5% correction, and up to double that in the large Q case. This can be an important correction, depending on the accuracy of the measurement. It represents a systematic error that may be swamped by other experimental

errors. However, from now on we shall ignore it, but keep in mind that large T and/or large Q analyses, with small masses, may be problematic, unless we adopt a relativistic correction.

Photons are always relativistic. So, if they are involved, we use $T_\gamma = E_\gamma$, and T_γ/c for its momentum.

Laboratory frame, non-relativistic analysis

In the laboratory frame, in a non-relativistic analysis, we make the following approximations:

1)	$T_a < 10 \text{ MeV}$	kinetic energy of the projectile
2)	$\vec{p}_a = p_a \hat{z}$	projectile's direction is along the positive z -axis
3)	$T_X = 0$	target is at rest
4)	$1 \leq m_a, m_b \leq 4u$	small mass projectile, observed particle
5)	$m_X, m_Y \geq 4u$	large mass target, unobserved particles
6)	$\gamma_i = 1$	no relativistic corrections

With these approximations, Conservation of Energy and Conservation of Linear Momentum can be expressed in the following equations:

$$Q + T_a = T_b + T_Y, \quad (17.12)$$

$$\vec{p}_a = \vec{p}_b + \vec{p}_Y. \quad (17.13)$$

Since the Y-particle is unobserved, we choose to eliminate it from the (17.12) and (17.13), with the result:

$$T_b(m_Y + m_b) - 2\sqrt{m_a m_b T_a} \cos \theta_b \sqrt{T_b} - [m_Y(Q + T_a) - m_a T_a] = 0. \quad (17.14)$$

This is a quadratic equation in $\sqrt{T_b}$, in terms of the (presumably) known quantities, T_a , Q , and the masses. Solving the quadratic equation yields:

$$T_b = \frac{\sqrt{m_a m_b T_a} \cos \theta_b \pm \sqrt{m_a m_b T_a \cos^2 \theta_b + (m_Y + m_b)[m_Y Q + (m_Y - m_a)T_a]}}{(m_Y + m_b)}. \quad (17.15)$$

Thus, we see through (17.14), that 2-body reactions involve a direct correlation of the scattering angle, θ_b and the b-particle's energy, T_b . Consequently, if one measures, T_b , and $\cos \theta_b$ is also determined. The relationship between the two differential cross sections is:

$$\frac{d\sigma}{d\Omega_b} = \frac{d\sigma}{d\phi_b dT_b} \left(\frac{dT_b}{d(\cos \theta_b)} \right), \quad (17.16)$$

or

$$\frac{d\sigma}{d\phi_b dT_b} = \frac{d\sigma}{d\Omega_b} \left(\frac{d(\cos \theta_b)}{dT_b} \right). \quad (17.17)$$

The derivatives inside the large parentheses in (17.16) and (17.17) may be worked out from (17.14) and (17.15).

(17.15) may be complicated, but is also very rich in physical content. Several interesting features should be noted:

1. If $Q > 0$, then

$$\sqrt{m_a m_b T_a} \cos \theta_b < \sqrt{m_a m_b T_a \cos^2 \theta_b + (m_Y + m_b)[m_Y Q + (m_Y - m_a)T_a]},$$

and, therefore, we must always choose the positive sign in (17.15).

2. If $Q < 0$, then there exists the possibility that, given a certain value of T_a , at an angle $\theta_b < \pi/2$, there can be two possible values of T_b . There is an energy threshold on T_a for this to occur. At threshold, $\theta_b = 0$, as demonstrated in Figure 17.3.

At this threshold, the $\sqrt{(\quad)}$ term vanishes. This implies that, at $T_a = T_{th}$, we have the condition:

$$0 = m_a m_b T_{th} \cos^2 \theta_b + (m_Y + m_b)[m_Y Q + (m_Y - m_a)T_{th}].$$

Solving for T_{th} gives:

$$T_{th} = \frac{-Q(m_Y + m_b)}{m_Y + m_b - m_a}. \quad (17.18)$$

3. Once $T_a > T_{th}$, there is an upper limit on T_a , called T'_a for this double-valued behavior on T_b . When $T_a = T'_a$, the smaller T_b falls to zero. This requires that:

$$\sqrt{m_a m_b T_a} \cos \theta_b = \sqrt{m_a m_b T_a \cos^2 \theta_b + (m_Y + m_b)[m_Y Q + (m_Y - m_a)T_a]},$$

from which we conclude that:

$$T'_a = \frac{-Q m_Y}{m_Y - m_a}. \quad (17.19)$$

Figure 17.3: Laboratory and center of momentum pictures of the X(a,b)Y interaction process.

4. For double-valued behavior on T_b , combining the results of (17.18) (17.19), we see that T_a must fall in the range:

$$\frac{m_Y + m_b}{m_Y + m_b - m_a} \leq \frac{T_a}{|Q|} \leq \frac{m_Y}{m_Y - m_a} . \quad (17.20)$$

5. If $T_{th} < T_a < T'_a$, there are also scattering angles for which double-valued behavior can not exist. This happens when the argument of the $\sqrt{\quad}$ falls to zero. This defines a maximum scattering angle for double-valued observation. From (17.15), we see that this maximum angle is given by:

$$\cos^2 \theta_b^{\max} = \frac{m_Y + m_m}{m_a m_b T_a} [-m_Y Q - (m_Y - m_a) T_a] \quad (17.21)$$

These concepts are illustrated in Krane's Figures 11.2(a) and 11.2(b) on pages 382–384, as well (eventually) in Figure 17.4.f

Figure 17.4: Demonstration of the double-valued nature of T_b .

Determining Q from scattering experiments

Up to now, we have assumed that Q was known. In some cases it is not, but, we can determine it from a scattering experiment. Reorganizing (17.14) as follows,

$$Q = T_b \left(1 + \frac{m_b}{m_Y} \right) - T_a \left(1 + \frac{m_a}{m_Y} \right) - 2 \cos \theta_b \left(\frac{m_a m_b}{m_Y^2} T_a T_b \right)^{1/2}, \quad (17.22)$$

appears that we have isolated Q . However, recalling the definition of Q ,

$$Q \equiv (m_a + m_x - [m_b + m_Y])c^2, \quad (17.23)$$

our lack of knowledge of Q is tantamount to not knowing, at least with sufficient accuracy, one (or more) of the masses. For this type of experiment, it is usually the case, that m_Y is the unknown factor. “X” is usually in the ground state, and hence, well characterized. “a”

and “b” are light particles with $A \leq 4$, and therefore, extremely well known. “Y” is often left in an excited state, and is not known. Its ground state mass may be well known, but not its excited state. So, to recover this situation, we solve for m_y in terms of Q , and substitute for m_y in (17.23). We also perform the analysis at $\theta_b = \pi/2$ so simplify the arithmetic. (This is not a necessary step, but it does save brain cells for more useful activities.)

The result is:

$$Q = T_b - T_a + \frac{(T_a m_a c^2 + T_b m_b c^2)}{[m_x c^2 + m_a c^2 - m_b c^2] - Q} . \quad (17.24)$$

The most common approach to solving (17.24) is to form a common denominator, and then solve the resulting quadratic equation for Q . An alternative is presented below, treating (17.24) as an iterative or recursive equation.

It goes as follows:

1. Define a time-saving shorthand:

$$Q = \delta + \frac{()}{[] - Q} , \quad (17.25)$$

where $\delta \equiv T_b - T_a$, and we have simply left the contents of the brackets empty. By using different types of brackets, we keep the symbols from getting mixed up. A clash of symbols is to be avoided.

2. Form the lowest order solution:

$$Q_0 = \delta + \frac{()}{[]} , \quad (17.26)$$

3. The n^{th} correction to Q is found from

$$\sum_{i=0}^n Q_i = \delta + \frac{()}{[] - \sum_{i=0}^{n-1} Q_i} , \quad (17.27)$$

4. The final answer is

$$Q = \sum_{i=0}^n Q_i . \quad (17.28)$$

The iteration is stopped when the answer is “good enough”.

Illustration:

$$\begin{aligned}
 Q_0 &= \delta + \frac{Q_0}{\Delta} \\
 Q_0 + Q_1 &= \delta + \frac{Q_0}{\Delta - Q_0} \\
 Q_0 + Q_1 &= \delta + \frac{Q_0}{\Delta} \left(\frac{1}{1 - Q_0/\Delta} \right) \\
 Q_0 + Q_1 &\cong \delta + \frac{Q_0}{\Delta} (1 + Q_0/\Delta) \\
 Q_0 + Q_1 &= Q_0 + Q_0(\delta)/\Delta^2 \\
 Q_1 &= Q_0(\delta)/\Delta^2
 \end{aligned} \tag{17.29}$$

Thus, the fractional correction is:

$$\frac{Q_1}{Q_0} = \frac{(T_a m_a c^2 + T_b m_b c^2)}{[m_x c^2 + m_a c^2 - m_b c^2]^2} . \tag{17.30}$$

In the worst possible case, $m_x = m_a = m_b \cong 4u$, and $T_a = T_b \cong 10$ MeV, giving $Q_1/Q_0 \cong 5 \times 10^{-3}$. Since Q -values are known typically to $\approx 1 \times 10^{-4}$, this can be an important correction, especially for small- A target nuclei.

17.3 Isospin

We know that the strong force does not distinguish between protons and neutrons (mostly). Therefore, one can consider this to be another kind "of symmetry", and symmetries have quantum numbers associated with them. Consider neutrons and protons to be two states of a more general particle, called the nucleon, a name we have used throughout our discussions. However, now associate a new quantum number called "isospin", with the symbol T_3 , and the following numerical assignments.

particle	T_3
p	$+\frac{1}{2}$
n	$-\frac{1}{2}$
${}^A_Z X_N$	$\frac{1}{2}(Z - N)$

Table 17.1: Isospin assignments

The assignment of the plus sign to the proton is completely arbitrary, but now part of convention.

Historically, isospin has been called *isotopic spin*, where a given Z, T_3 combination identifies a specific isotope associated with Z , or *isobaric spin*, where a given A, T_3 combination identifies a specific isobar associated with A . Today, "isospin" appears to be the preferred name.

As long as the strong force does not distinguish between isobars associated with a given A , we expect to see some similarity in the excitation levels associated with nuclei with the same A . There is evidence for this, as seen in Figure 11.5 in Krane.

Isospins combine just as regular spins do. This is seen in the following example:

The dinucleon

Let us now consider the possible ways of combining two nucleons. We form the composite wavefunctions for two nucleons, one with spatial wavefunction $\psi(\vec{x}_1)$ and one with spatial wavefunction $\psi(\vec{x}_2)$. We label these as nucleon "1" and "2". We also include their isospin as either up, \uparrow , or down, \downarrow . Finally, since they are intrinsic spin- $\frac{1}{2}$ particles, they must obey the Pauli Exclusion Principle, and form composite wavefunctions that are antisymmetric under the exchange of quantum numbers. Doing so, results in:

Note that the parity is associated with the space part of the wavefunction only. Also note, that the difference between the observed deuteron and its odd parity counterpart (unobserved) is how the antisymmetry is achieved. In the unobserved case, it is the spatial part that is antisymmetrized, while the observed deuteron has a positive parity spatial wavefunction and an antisymmetrized isospin wavefunction. In order to make full use of the attractive strong force, the nucleons must come into close proximity. All of the members of the isobaric

T	T_3	composite wavefunction	π	
1	1	$2^{-1/2}[\psi_1(\vec{x}_1)\psi_2(\vec{x}_2) - \psi_1(\vec{x}_2)\psi_2(\vec{x}_1)](\uparrow_1\uparrow_2)$	-1	diproton
1	0	$2^{-1}[\psi_1(\vec{x}_1)\psi_2(\vec{x}_2) - \psi_1(\vec{x}_2)\psi_2(\vec{x}_1)](\uparrow_1\downarrow_2 + \downarrow_1\uparrow_2)$	-1	odd parity deuteron?
1	-1	$2^{-1/2}[\psi_1(\vec{x}_1)\psi_2(\vec{x}_2) - \psi_1(\vec{x}_2)\psi_2(\vec{x}_1)](\downarrow_1\downarrow_2)$	-1	dineutron
0	0	$2^{-1}[\psi_1(\vec{x}_1)\psi_2(\vec{x}_2) + \psi_1(\vec{x}_2)\psi_2(\vec{x}_1)](\uparrow_1\downarrow_2 - \downarrow_1\uparrow_2)$	+1	Deuteron

Table 17.2: The dinucleon quantum states

triplet have antisymmetric spatial wavefunctions. That is why none are bound.

17.4 Reaction Cross Sections

Covered elsewhere, and partly in 311.

17.5 Experimental Techniques

Not covered in 312.

17.6 Coulomb Scattering

Covered in 311.

17.7 Nuclear Scattering

Covered in Chapter 10.

17.8 Scattering and Reaction Cross Sections

Consider a \hat{z} -direction plane wave incident on a nucleus, as depicted in Figure 17.5.

The wavefunction for the incident plane wave:

$$\psi_{\text{inc}} = Ae^{ikz} . \quad (17.31)$$

Figure 17.5: Scattering of a plane wave from a nucleus.

We have seen elsewhere, that (17.31) is a solution to the Schrödinger equation in a region of space where there is no potential (or a constant potential). Since no potential is also a central potential (in the sense that it does not depend on orientation), we should be able to recast the solution in spherical-polar coordinates, and identify the angular momentum components of the incident wave. If we did this, we could show:

$$\psi_{\text{inc}} = Ae^{ikz} = A \sum_{l=0}^{\infty} i^l (2l+1) j_l(kr) P_l(\cos \theta) . \quad (17.32)$$

The j_l 's are the “spherical Bessel functions, and the P_l 's are the regular Legendre polynomials, that we have encountered before.

The properties of the j_l 's are:

$$\begin{aligned}
j_0(z) &= \frac{\sin z}{z} \\
j_1(z) &= \frac{\sin z}{z^2} - \frac{\cos z}{z} \\
j_2(z) &= \frac{3 \sin z}{z^3} - \frac{3 \cos z}{z^2} - \frac{\sin z}{z} \\
j_l(z) &= (-z)^l \left(\frac{1}{z} \frac{d}{dz} \right)^l j_0(z) \\
\lim_{z \rightarrow 0} j_l(z) &= \frac{z^l}{(2l+1)!!} + \mathcal{O}(z^{l+1}) \\
\lim_{z \rightarrow \infty} j_l(z) &= \frac{\sin(z - l\pi/2)}{z} + \mathcal{O}(z^{-2})
\end{aligned} \tag{17.33}$$

Thus, we have identified the angular momentum components of the incoming wave, with angular momentum components $l\hbar$. The magnetic quantum number associated with l , namely, m_l does not appear in (17.32) because (17.31) has azimuthal symmetry. This is not a requirement, and is easy to account for, but is not required for our discussions. (17.33) is called the “partial wave expansion”, and exploiting it to extract physical results is called “partial wave analysis”.

17.8.1 Partial wave analysis

Semi-classical introduction

As an introduction to this section, first let’s estimate the cross section of a nucleus, using semi-classical physics. We know, from classical scattering analysis, that the impact parameter, b , is associated with the angular momentum of the projectile about the target, centered at the origin. Equating the quantum mechanical angular momentum of the wave component with its classical counterpart, we get:

$$pb = l\hbar, \tag{17.34}$$

or

$$b = \frac{l\hbar}{p} = \frac{l}{2\pi} \frac{h}{p} = l \frac{\lambda}{2\pi} = l\lambda, \tag{17.35}$$

in terms of the reduced wavelength, λ .

So, continuing with this semiclassical train of thought:

$l = 0 \rightarrow 1$ covers the area $\pi\lambda^2$

$l = 1 \rightarrow 2$ covers the area $(4 - 1)\pi\lambda^2$

$l \rightarrow l + 1$ covers the area $[(l + 1)^2 - l^2]\pi\lambda^2 = (2l + 1)\pi\lambda^2$

Summing up all these contributions:

$$\sigma = \sum_{l=0}^{[R/\lambda]} (2l + 1)\pi\lambda^2 = \pi(R + \lambda)^2, \quad (17.36)$$

where R is the nuclear radius. Thus, we see that λ factors into the computation of the cross section as an effective size of the projectile.

The quantum approach

We start by recognizing that we wish to consider the mathematic representation of the wave at locations far from the scattering center. Thus, for $kr \gg 1$, we use the asymptotic result of (17.33),

$$\lim_{kr \rightarrow \infty} j_l(kr) = \frac{\sin(kr - l\pi/2)}{kr} = i \frac{[e^{-i(kr - l\pi/2)} - e^{i(kr - l\pi/2)}]}{2kr}. \quad (17.37)$$

Combining (17.36) with (17.32) gives,

$$\psi_{\text{inc}} = Ae^{ikz} = \frac{A}{2kr} \sum_{l=0}^{\infty} i^{l+1} (2l + 1) [e^{-i(kr - l\pi/2)} - e^{i(kr - l\pi/2)}] P_l(\cos \theta). \quad (17.38)$$

This is an interesting result! The $e^{-ikr}/(kr)$ part represents a spherical wave converging on the nucleus, while the $e^{ikr}/(kr)$ part represents a spherical wave moving away from the nucleus. The nucleus can only modify the outgoing part. One way of representing this is via a modification of the outgoing part. Thus, the total solution, with incoming and scattered parts, is written:

$$\psi = Ae^{ikz} = \frac{A}{2kr} \sum_{l=0}^{\infty} i^{l+1} (2l + 1) [e^{-i(kr - l\pi/2)} - \eta_l e^{i(kr - l\pi/2)}] P_l(\cos \theta), \quad (17.39)$$

where η_l is a complex coefficient that represents the mixing the two parts of the outgoing wave, part of which is associated with the initial plane wave, as well as the scattered part. Thus, the total wave is a combination of both,

$$\psi = \psi_{\text{inc}} + \psi_{\text{sc}}, \quad (17.40)$$

allowing us to express the scattered part by itself,

$$\psi_{\text{sc}} = \frac{Aie^{ikr}}{2kr} \sum_{l=0}^{\infty} (2l+1)(1-\eta_l)P_l(\cos\theta) . \quad (17.41)$$

As in 1D, we use the probability current density to evaluate the effectiveness of the scatterer. The scattered probability current is:

$$j_{\text{sc}} = \frac{\hbar}{2im} \left[\psi_{\text{sc}}^* \left(\frac{\partial \psi_{\text{sc}}}{\partial r} \right) - \left(\frac{\partial \psi_{\text{sc}}^*}{\partial r} \right) \psi_{\text{sc}} \right] . \quad (17.42)$$

Putting (17.41) into (17.42) results in:

$$j_{\text{sc}} = |A|^2 \left(\frac{\hbar}{4kr^2} \right) \left| \left[\sum_{l=0}^{\infty} (2l+1)(1-\eta_l)P_l(\cos\theta) \right] \right|^2 . \quad (17.43)$$

Since the incoming wave has probability current

$$j_{\text{inc}} = \frac{\hbar k}{m} , \quad (17.44)$$

the differential cross section is expressed as follows:

$$\frac{d\sigma}{d\Omega} = \frac{j_{\text{sc}}}{j_{\text{inc}}} r^2 , \quad (17.45)$$

in analogy with the 1D transmission and reflection coefficients.

Then, we can show that

$$\frac{d\sigma_{\text{sc}}}{d\Omega} = \frac{1}{4k^2} \left| \sum_{l=0}^{\infty} (2l+1)(1-\eta_l)P_l(\cos\theta) \right|^2 , \quad (17.46)$$

and

$$\sigma_{\text{sc}} = \frac{\pi}{k^2} \sum_{l=0}^{\infty} (2l+1)|1-\eta_l|^2 . \quad (17.47)$$

Since both the incident and outgoing waves have wavenumber k , the cross sections discussed above model “elastic” scattering. Elastic scattering is characterized by no loss of probability of the incoming particle. Mathematically, this is expressed by,

$$|\eta_l| = 1 ,$$

for all l . Thus, the only thing that the target does is to redirect the wave and shift its phase. Hence we, define a *phase shift*, δ_l , for each l -component, using the following convention,

$$\eta_l = e^{2i\delta_l} ,$$

from which we can derive:

$$\sigma_{\text{sc}}^{\text{elas}} = 4\pi\lambda^2 \sum_{l=0}^{\infty} (2l+1) \sin^2 \delta_l . \quad (17.48)$$

From now on, we'll reserve the name, σ_{sc} for elastic scattering only. Note that $1/k = \lambda/(2\pi) \equiv \lambda$.

Reaction cross sections

Generally, however, $|\eta_l| < 1$, as the incoming beam can be absorbed, and part of it unabsorbed. We will identify:

$$\frac{d\sigma_r}{d\Omega} = \frac{j_{\text{in}} - j_{\text{out}}}{j_{\text{inc}}} r^2 , \quad (17.49)$$

as the *reaction* cross section, involving the difference between the currents of the incoming and outgoing spherical waves.

From (17.38) we see that:

$$\begin{aligned} \psi_{\text{in}} &= \frac{A}{2kr} \sum_{l=0}^{\infty} i^{2l+1} (2l+1) [e^{-i(kr-l\pi/2)}] P_l(\cos\theta) \\ &= \frac{Aie^{-ikr}}{2kr} \sum_{l=0}^{\infty} i^{2l} (2l+1) P_l(\cos\theta) \end{aligned} \quad (17.50)$$

$$\begin{aligned} \psi_{\text{out}} &= -\frac{A}{2kr} \sum_{l=0}^{\infty} i^{2l} (2l+1) \eta_l [e^{i(kr-l\pi/2)}] P_l(\cos\theta) \\ &= \frac{-Aie^{ikr}}{2kr} \sum_{l=0}^{\infty} (2l+1) \eta_l P_l(\cos\theta) . \end{aligned} \quad (17.51)$$

Adapting (17.42) we obtain the incoming and outgoing probability currents:

$$j_{\text{in}} = |A|^2 \left(\frac{\hbar}{4kr^2} \right) \left| \left[\sum_{l=0}^{\infty} i^{2l} (2l+1) P_l(\cos \theta) \right] \right|^2 \quad (17.52)$$

$$j_{\text{out}} = |A|^2 \left(\frac{\hbar}{4kr^2} \right) \left| \left[\sum_{l=0}^{\infty} (2l+1) \eta_l P_l(\cos \theta) \right] \right|^2 \quad (17.53)$$

Combining (17.49) with (17.44), (17.52) and (17.53), and then integrating over all angles, results in:

$$\sigma_{\text{r}} = \pi \lambda^2 \sum_{l=0}^{\infty} (2l+1) (1 - |\eta_l|^2) . \quad (17.54)$$

Note that for elastic scattering, $\sigma_{\text{r}} = 0$.

Total cross section

The total cross section is the sum of the inelastic and reaction cross sections. Adding (17.47) and (17.54) result in:

$$\sigma_{\text{t}} = \sigma_{\text{sc}} + \sigma_{\text{r}} = 2\pi \lambda^2 \sum_{l=0}^{\infty} (2l+1) [1 - \Re(\eta_l)] , \quad (17.55)$$

where $\Re()$ is some typesetting software's idea of "real part".

Our results are summarized in the following table, for the contribution to the cross sections from the l 'th partial wave.

Process	η_l	$\sigma_{\text{sc}}^l / (\pi \lambda^2 (2l+1))$	$\sigma_{\text{r}}^l / (\pi \lambda^2 (2l+1))$	
elastic only	$ \eta_l = 1$	$ 1 - \eta_l ^2$	0	no loss of probability
absorption only	$\eta_l = 0$	1	1	equal!
Mixed	$\eta_l = ?$	$ 1 - \eta_l ^2$	$1 - \eta_l ^2$	work to do!

The most interesting feature is, that even with total absorption of the l 'th partial wave, elastic scattering is predicted. This is because waves will always (eventually) fill in the shadow region behind an absorber. A good way to demonstrate this for yourself, is to hold a pencil near the ground, on one of those rare sunny days in Michigan. Near the ground, the shadow is sharp, well-defined. As you raise the pencil the edges become fuzzy. Eventually, if you hold it high enough, its shadow disappears entirely.

How are the partial wave amplitudes are computed?

Although the foregoing analysis is elegant, we still have considerable work to do for the general case. For the theoreticians amongst us, we have to solve the radial Schrödinger equation for the potential that causes the scattering (assuming it's a central potential) and guarantee slope and value continuity everywhere. The η_i 's are then determined the asymptotic forms of the solutions. Typically a numerical procedure is followed. For the experimentalists among us, the differential cross sections have to be mapped out, and the η_i 's are inferred by inverting equations (17.46) as well as its reaction counterpart. Fortunately, for nuclear scattering, only the first few partial waves are important. Interested readers should consult Krane's book, Section 4.2 for more details.

17.9 The Optical Model

The optical model of the nucleus employs a model of the nucleus that has a complex part to its potential. Calling this generalized potential, $U(r)$, we have the definition:

$$U(r) = V(r) - iW(r) , \quad (17.56)$$

where $V(r)$ is the usual attractive potential (treated as a central potential in the optical model), and its imaginary part, $W(r)$, where $W(r)$ is real and positive. The real part is responsible for elastic scattering, while the imaginary part is responsible for absorption. (With a plus sign, in (17.56), this can even be employed to model probability increase (particle creation), but I have never seen it employed in this fashion.)

The theoretical motivation for this approach comes from the continuity relationship for Quantum Mechanics (derived in NERS311):

$$\frac{\partial P}{\partial t} + \vec{\nabla} \cdot \vec{S} = \frac{2}{\hbar} \Psi^* \Im(U\Psi) , \quad (17.57)$$

where P is the probability density, \vec{S} is the probability current density, and $\Im()$ is some typesetting software's idea of "imaginary part". When the potential is real, probability is conserved, the left-hand side of (17.57) expressing the balance between probability and where it's moving. (This is really the transport equation for probability.) When the imaginary part is negative, loss of probability is described. When the imaginary part is positive, (17.57) describes probability growth.

The potentials that are used for optical modeling are:

$$\begin{aligned} V(r) &= \frac{-V_0}{1 + e^{(r-R_N)/a}} , \\ W(r) &= dV/dr , \end{aligned} \quad (17.58)$$

where R_N is the nuclear radius, a is the skin depth, and $-V_0$ is the potential at the center of the nucleus (almost). These are plotted in Figure 17.6

Figure 17.6: The optical model potentials

This is a clever choice for the absorptive part. The absorption can only happen at the edges of the nucleus where there are vacancies in the shells (at higher angular momentum).

See Figures 11.17 and 11.18 in Krane.

17.10 Compound-Nucleus Reactions

See Figure 17.7.

In this reaction, projectile “ a ”, enters the nucleus with a small impact parameter (small value of l). It interacts many times inside the nucleus, boosting individual nucleons into excited states, until it comes to rest inside the nucleus. This “compound nucleus” has too much energy to stay bound, and one method it may employ is to “boil off” nucleons, to

Figure 17.7: Schematic of a compound nucleus reaction

reach stability. One, two, or more nucleons can be shed. The nucleons that are boiled off, are usually neutrons, because protons are reflected back inside, by the Coulomb barrier. Symbolically, the reaction is:



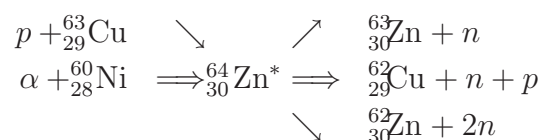
The resultant light particle b_i can represent one or more particles.

In this model, the reaction products lose track of how the compound nucleus was formed. The consequences and restrictions of this model are:

1. Different initial reactants, $a + X$ can form the same C^* with the same set of decays. Once the projectile enters the nucleus it loses identity and shares its nucleons with C^* . It should not matter how C^* is formed. Figure 11.19 in Krane shows how different ways of creating ${}_{30}^{64}\text{Zn}^*$ leads (mostly) to the same cross sections for each decay channel.

2. The b_i are emitted isotropically (since the compound nucleus loses sense of the initial direction of a , since it scatters many times within the compound nucleus and “isotropises”. This is especially important when the projectile is light, and the angular momentum not too high. See Figure 11.20 in Krane for experimental evidence of this.
3. Initial projectile energies are generally in the range 10–20 MeV, and X is usually a medium or heavy nucleus. This is so that the projectile can not exit the nucleus with its identity, and some of its initial kinetic energy, intact.
4. In order for the compound nucleus to form, it needs substantial time to do so, typically, 10^{-18} – 10^{-16} s.

As an example:



Heavy projectile (such as α -particle’s) with large l exhibit compound nucleus decays that have a completely different signature. The b_i ’s are generally emitted in the forward and backward direction, as both the angular momentum and angular momentum must be conserved. As the projectile energy increases, one can see more neutrons being emitted in proportion. Krane’s Figure 11.21 illustrates this very well.

17.11 Direct Reactions

A “direct reaction” involves a projectile that is energetic enough to have a reduced wavelength, λ , of the order of 1 fm (a 20 MeV nucleon, for example), that interacts in the periphery of the nucleus (where the nuclear density starts to fall off), and interacts with single valence nucleon. That single nucleon interacts with the projectile leaving them both in bound, but unstable orbits. This state typically lives for about 10^{-21} s, which is long enough for the valence nucleon and projectile to (in classical terms) make several round trips around the nucleus, before one of them finds a way to escape, possibly encountering the Coulomb barrier along the way. Since angular and linear momentum must be conserved, the ejected particle is generally ejected into the forward direction.

Krane shows some interesting data in his Figure 11.19, where both the compound nucleus cross section and direct reaction cross section for ${}^{25}\text{Mg}(p, p)\text{Mg}^{25}$ are plotted, having been obtained from measurements. The compound nucleus interaction is seen to be nearly isotropic,

while the direct reaction is peaked prominently in the forward direction. The measurement makes use of the different lifetimes for these reactions, to sort out the different decay modes.

A (p, p) direct reaction, if the nucleus is left in its ground state, is an elastic collision. The same may be said for (n, n) collisions. If the nucleus is left in an excited state, it is an inelastic collision. (p, p) and (n, n) direct reactions are sometimes called “knock-out” collisions. Other examples of inelastic direct reaction collisions are (n, p) and (p, n) knock-out collisions. Yet other examples are “deuteron stripping” reactions, (d, p) or (d, n) , and “ α -stripping” reactions, (α, n) and (α, p) . The inverse reactions are also possible, (p, d) , (n, d) , (n, α) , (p, α) , and so on. These are called “pick-up” reactions. Measurements of inelastic direct reaction with light projectiles are very useful for determining the nuclear structure of excited states.

17.12 Resonance Reactions

We learned most of what we need to know intuitively about resonance reactions, from our discussion, in NERS311, regarding the scattering of waves from finite-size, finite-depth barriers. Recalling those results, for a particle wave with particle mass, m , energy, E incident on a potential well, $V = -V_0$ between $-R \leq z \leq R$, and zero everywhere else, the transmission coefficient turns out to be:

$$T = \frac{1}{1 + \frac{V_0^2}{4E(E+V_0)} \sin^2(2KR)} , \quad (17.59)$$

where $K = \sqrt{2m(E + V_0)}/\hbar$. We note that the transmission coefficient is unity, when $2KR$ is a multiple of π . This is called a resonance. Resonances are depicted in Figure 17.8 for neutrons incident on a potential with depth, $V = 40$ MeV, and nuclear radius, $R = 3.5$ fm. Note the dense population of resonant lines. Figure 17.9 isolates only one of these resonances.

In 3 dimensions the analogous thing happens. In fact, it resonances are common everyday occurrence. All it requires is a bound state that has a given frequency, that can be matched by an external identical, or nearby frequency. All radios work this way. Unbounded radio waves are received by antennae that have bound-state frequencies that match. That’s a good resonance. Good resonances are responsible for a piano’s rich tone. If you look ”underneath the hood” of a piano, you may have wondered why some hammers hit 3 strings simultaneously (upper registers), two strings in the middle registers, and one in the bass registers. These nearby strings, grouped at the same pitch, when struck together, cause sympathetic vibrations and overtones that add to the rich sound. Strings of different pitches can interact as well. For example, try the following (on an acoustic piano): Strike A4 (440 Hz the A above middle C) quite hard, and then hold down the damper pedal, if your hearing acuity is quite good, you may start to hear E5 ($659.26 = 1.4983 \times 440$ Hz, a fifth above A4) start to

ring, and then, possibly, C#6 (an octave plus a third above A4, $1108.73 = 2.5198 \times 440$ Hz). Both are near half-integral multiples of 440, and are close enough to resonate. You may have wondered why old-school piano technicians can tune an entire piano, with one tuning fork (A4). A4 is tuned against the fork, then E5, and so on, in increments of fifths and octaves, until the job is complete.

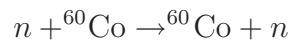
Returning now, to nuclei, it is the same effect, except that the bound-state frequencies are defined by the quantum mechanical solutions to the Schrödinger equation. It does not matter that a level is unoccupied. If a passing free neutron has the right energy (frequency), that level will ring, and cause a sharp spike in the cross section.

Shape of a resonance

We can use our partial wave analysis to analyze this. Starting with (17.55):

$$\sigma_t = \sigma_{sc} + \sigma_r = 2\pi\lambda^2 \sum_{l=0}^{\infty} (2l+1)[1 - \Re(\eta_l)] . \quad (17.60)$$

For illustrative purposes we shall consider the resonance



that has a known resonance in the vicinity of $E_n = 130$ keV.

In this case,

$$\lambda = \frac{\hbar c}{\sqrt{2m_n c^2 T}} \approx 400\text{fm} ,$$

a reduced wavelength that is considerably larger than the nucleus.

Let us imagine that just one of the η_l 's is causing the resonance. From (17.60). we see that σ_t maximizes when $\Re(\eta_l) = -1$. Also, considering that this resonance we'll model as an elastic process, we set

$$\eta_l = -1 = e^{2i\delta_l} \Rightarrow \delta_l = \pi/2 .$$

To determine the shape of the resonance, we shall expand the phase shift in the vicinity of E_n , where $\delta_l(E_n = E_{res}) = \pi/2$.

Doing so,

$$\cot \delta_l(E_n) \rightarrow \cot \delta_l(E_n) \Big|_{\delta_l(E_{res})=\pi/2} + (E_n - E_{res}) \frac{\partial \cot \delta_l(E_n)}{\partial E_n} \Big|_{E_n=E_{res}} + \dots$$

$$\frac{\partial \cot \delta_l(E_n)}{\partial E_n} = -\frac{\partial \delta_l(E_n)}{\partial E_n} - \frac{\cos^2 \delta_l(E_n)}{\sin \delta_l(E_n)} \frac{\partial \delta_l(E_n)}{\partial E_n}$$

The second term vanishes above. Defining

$$\Gamma = 2 \left(\frac{\partial \delta_l(E_n)}{\partial E_n} \right)^{-1} \Big|_{E_n = E_{\text{res}}},$$

we have, from the above,

$$\cot \delta_l(E_n) = -\frac{E_n - E_{\text{res}}}{\Gamma/2}, \quad (17.61)$$

Since,

$$\sin(\delta_l) = \frac{1}{\sqrt{1 + \cot^2(\delta_l)}},$$

we have

$$\sin \delta_l = \frac{\Gamma/2}{[(E_n - E_{\text{res}})^2 + \Gamma^2/4]^{1/2}}. \quad (17.62)$$

Finally, combining (17.62) with (17.48)

$$\sigma_{\text{sc}}^{\text{el}}(E_n) = \pi \lambda^2 (2l + 1) \frac{\Gamma^2}{[(E_n - E_{\text{res}})^2 + \Gamma^2/4]}. \quad (17.63)$$

At resonance,

$$\sigma_{\text{sc}}^{\text{el}}(E_n) = 4\pi \lambda^2 (2l + 1). \quad (17.64)$$

In this example, $\lambda \approx 200$ fm, giving a resonant cross section of about $200(2l + 1)$ barns. recalling that the cross section area of a typical nucleus is about $1 b$, this is enormous!

What we have calculated so far is only for the case where there is one exit mode for the



resonance.

Gregory Breit and Eugene Wigner generalized (17.63) as follows:

$$\sigma_{\text{sc}}^{\text{el}}(E_n; [X(a, a)X]) = \pi\lambda^2 \frac{2I + 1}{(2s_a + 1)(2s_x + 1)} \frac{\Gamma_{aX}^2}{[(E_n - E_{\text{res}})^2 + \Gamma^2/4]} \quad (17.65)$$

$$\sigma_{\text{sc}}^{\text{in}}(E_n; [X(a, b_i)Y_i]) = \pi\lambda^2 \frac{2I + 1}{(2s_a + 1)(2s_x + 1)} \frac{\Gamma_{aX}\Gamma_{b_iY_i}}{[(E_n - E_{\text{res}})^2 + \Gamma^2/4]} \quad (17.66)$$

The I in the above equations comes from the coupling of the intrinsic spins of the reactants with the orbital angular momentum of the outgoing wave component,

$$\vec{I} = \vec{s}_x + \vec{s}_a + \vec{l}.$$

Γ in the denominator of both expressions above, pertains to the sum of all the partial widths of all the decay modes:

$$\Gamma = \sum_i \Gamma_i.$$

The factors Γ_{aX} and $\Gamma_{b_iY_i}$ in the above equations, pertain to the partial interaction probabilities for resonance formation, Γ_{aX} and decay, Γ_{aX} , in the case of one of the elastic channels, or $\Gamma_{b_iY_i}$.

Shape-elastic scattering

Resonant scattering rarely takes place in isolation, but in addition to other continuous elastic scattering, such as Rutherford scattering from a potential. If we call the potential scattering phase-shift, δ_l^{P} , one can show, from (17.47), that:

$$\sigma_{\text{sc}} = \pi\lambda^2(2l + 1) \left| e^{-2\delta_l^{\text{P}}} - 1 + i \frac{\Gamma}{(E_n - E_{\text{res}}) + i\Gamma/2} \right|^2. \quad (17.67)$$

Far from the resonance, the resonance dies out, and the cross section has the form:

$$\sigma_{\text{sc}} \longrightarrow 4\pi\lambda^2(2l + 1) \sin^2 \delta_l^{\text{P}},$$

while at the resonance, the resonance dominates and we have:

$$\sigma_{\text{sc}} \approx 4\pi\lambda^2(2l + 1).$$

In the vicinity of the resonance, the Lorentzian shape is skewed, with a “dip” for $E < E_{\text{res}}$, that arises from destructive interference between the potential and resonance phases. See Krane’s Figures 11.27 and 11.28 for examples of these.

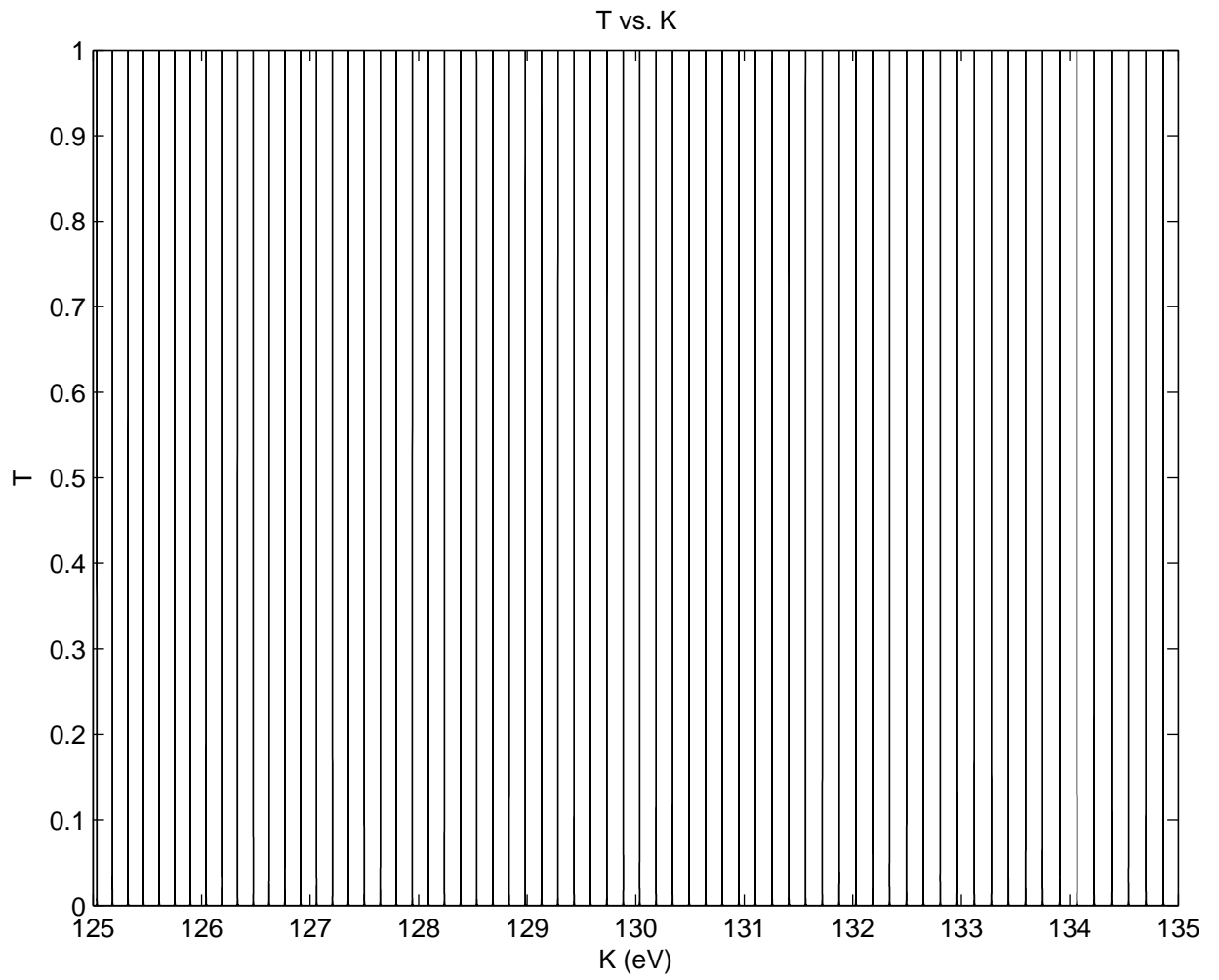


Figure 17.8: Resonant structure for an incident neutron. In this case, $V_0 = 40$ MeV, $R = 3.5$ fm.

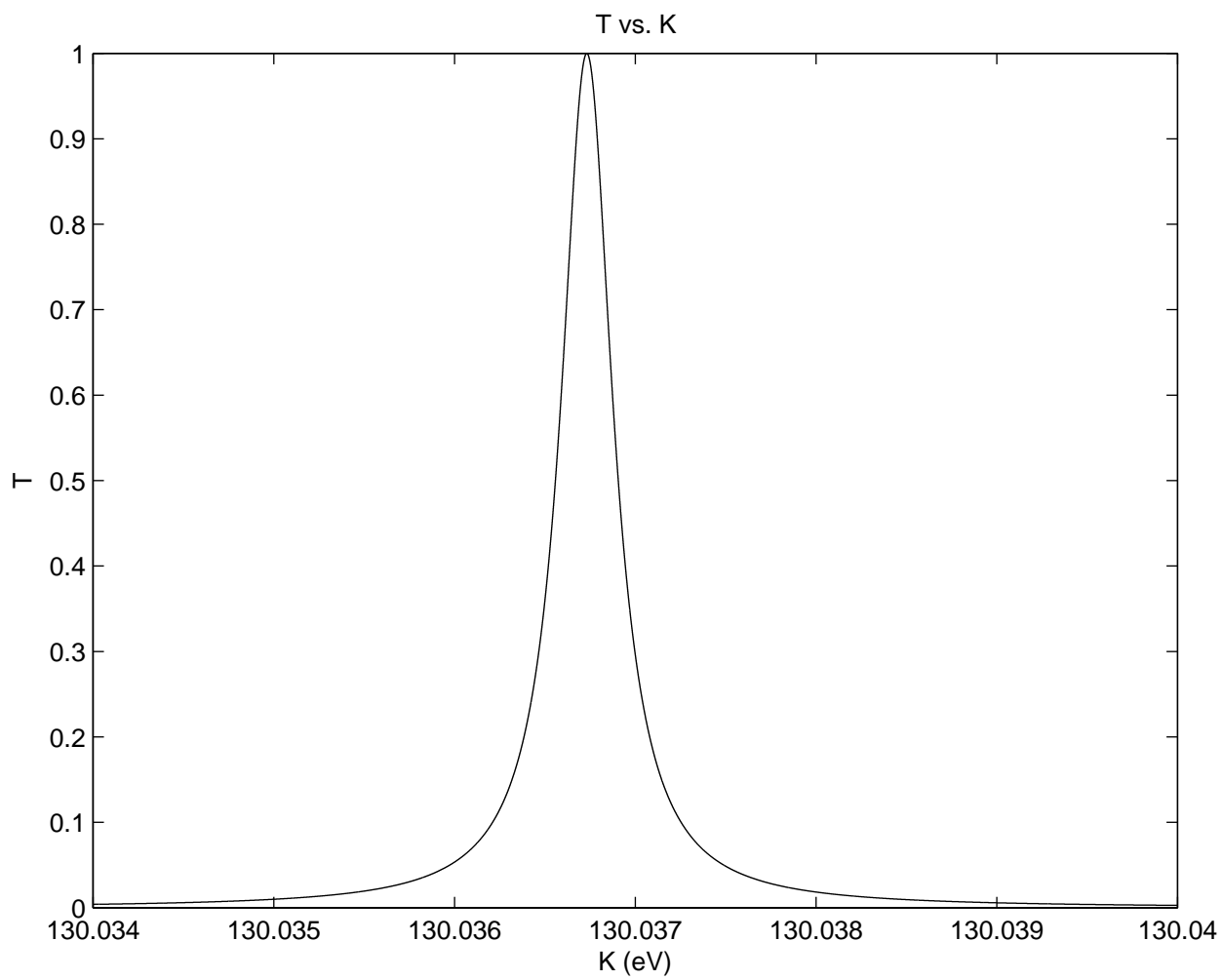


Figure 17.9: Resonant structure near one of the peaks.

Problems

1. Derive (17.10).
2. Derive (17.11).
3. Derive (17.14) and (17.15).
4. Work out the derivatives inside the large parentheses in (17.16) and (17.17).
5. Solve the quadratic equation implied by (17.24).
6. Work out Q_2 in (17.27).
7. Derive (17.47).
8. Derive (17.48).
9. The screened Rutherford cross section, differential in solid angle, is often used to describe the angular distribution of light charged particles scattering elastically from heavy nuclei. It has the following form:

$$\frac{d\sigma}{d\Omega} = \frac{A}{(1 - \cos\theta + a)^2} ,$$

where A and a are constants for any nucleus-projectile combination. The total cross section is known to be σ_0 .

(a) Show that:

$$A = \sigma_0 \frac{a(2+a)}{4\pi} .$$

(b) If the forward ($\theta = 0$) intensity is 10^6 times greater than that in the backward direction ($\theta = \pi$), show that:

$$a = \frac{2}{999} .$$

(c) If the forward ($\theta = 0$) intensity is 4 times greater than that in the backward direction ($\theta = \pi$), Show that:

$$a = 2 .$$

(d) In the limit that $a \rightarrow \infty$, show that the cross section is isotropic.

10. In the $X(a,b)Y$ reaction with known Q and X at rest, it was shown that:

$$T_b^{1/2} = \frac{(m_a m_b T_a)^{1/2} \cos\theta \pm \{m_a m_b T_a \cos^2\theta + (m_Y + m_b)[m_Y Q + (m_Y - m_a)T_a]\}^{1/2}}{m_Y + m_b} .$$

Show that:

- (a) When $Q < 0$, there is a minimum value of T_a for which the reaction is not possible. Show that this threshold energy is given by:

$$T_{\text{th}} = (-Q) \frac{m_Y + m_b}{m_Y + m_b - m_a} .$$

- (b) When $Q < 0$, and $T_a > T_{\text{th}}$, T_b can take on two values. The maximum T_a that this can occur is called T'_a . Show that:

$$T'_a = (-Q) \frac{m_Y}{m_Y - m_a} .$$

11. Projectile A , that has mass M_A , scatters elastically off of target nucleus X , that has mass M_X . $Q = 0$, and there is no exchange of matter.

- (a) Find a relationship between A 's magnitude of momentum, and its angle of deflection.

- (b) Show that there is a maximum scattering angle only when $m_A > m_X$.

- (c) Find the expression for this maximum angle, when $m_A > m_X$.